Hydron Transfer Catalyzed by Triosephosphate Isomerase. Products of Isomerization of (*R*)-Glyceraldehyde 3-Phosphate in D_2O[†]

AnnMarie C. O'Donoghue, Tina L. Amyes, and John P. Richard*

Department of Chemistry, University at Buffalo, SUNY, Buffalo, New York 14260-3000

Received September 22, 2004; Revised Manuscript Received December 1, 2004

ABSTRACT: The product distributions for the reactions of (*R*)-glyceraldehyde 3-phosphate (GAP) in D_2O at pD 7.5−7.9 catalyzed by triosephosphate isomerase (TIM) from chicken and rabbit muscle were determined by ^{1}H NMR spectroscopy. Three products were observed from the reactions catalyzed by TIM: dihydroxyacetone phosphate (DHAP) from isomerization with intramolecular transfer of hydrogen (49% of the enzymatic products), [1(*R*)-^{2}H]-DHAP from isomerization with incorporation of deuterium from D_2O into C-1 of DHAP (31% of the enzymatic products), and [2(*R*)-^{2}H]-GAP from incorporation of deuterium from D_2O into C-2 of GAP (21% of the enzymatic products). The similar yields of [1(*R*)-^{2}H]-DHAP and [2(*R*)-^{2}H]-GAP from partitioning of the enzyme-bound enediol(ate) intermediate between hydron transfer to C-1 and C-2 is consistent with earlier results, which showed that there are similar barriers for conversion of this intermediate to the α-hydroxy ketone and aldehyde products (Knowles, J. R., and Albery, W. J. (1977) *Acc. Chem. Res. 10*, 105−111). However, the observation that the TIM-catalyzed isomerization of GAP in D_2O proceeds with 49% intramolecular transfer of the ^{1}H label from substrate to product DHAP stands in sharp contrast with the ≤6% intramolecular transfer of the ^{3}H label from substrate to product GAP reported for the TIM-catalyzed reaction of [1(*R*)-^{3}H]-DHAP in H_2O (Herlihy, J. M., Maister, S. G., Albery, W. J., and Knowles, J. R. (1976) *Biochemistry 15*, 5601−5607). The data show that the hydron bound to the carboxylate side chain of Glu-165 in the TIM−enediol(ate) complex is *not* in chemical equilibrium with those of bulk solvent.

Triosephosphate isomerase (TIM)[1] catalyzes the stereospecific reversible 1,2-hydrogen shift at dihydroxyacetone phosphate (DHAP) to give (*R*)-glyceraldehyde 3-phosphate (GAP) by a single-base (Glu-165) proton-transfer mechanism through an enzyme-bound cis-enediol(ate) intermediate (Scheme 1) (*1*, *2*). The enzyme's low molecular weight (dimer, 26 kDa/subunit), high cellular abundance (*3*), and the centrality of proton transfer at carbon in metabolic processes (*4*, *5*) have made TIM a prominent target for studies on the mechanism of enzyme action. Consequently, the emergence of new experimental methods for the investigation of enzymatic reaction mechanisms, such as the use of tritium in tracer levels to monitor hydron transfer (*1*), Fourier transform infrared spectroscopy (*6*), NMR spectroscopy (*7*−*10*), X-ray crystallography (*11*−*13*), site-directed (*14*) and random mutagenesis (*15*), computational modeling (*16*−*20*), and the design and use of transition state analogue inhibitors (*21*, *22*) can be traced through studies on TIM.

Scheme 1

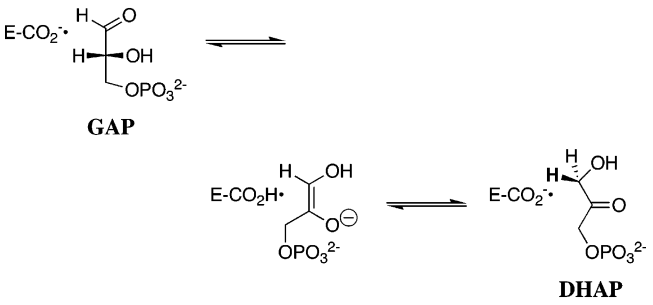

This work has shown that TIM approaches "perfection" in its catalysis of the isomerization of triose phosphates (*2*, *23*), and it has provided a detailed description of the chemical events that occur at the enzyme active site.

The chemical mechanism for proton transfer at the active site of TIM (*2*) is similar to that observed for the corresponding nonenzymatic isomerization reaction in water (*24*). Thus, the carboxylate anion side chain of Glu-165 functions as a Brønsted base to abstract a proton from the α-carbonyl carbon of bound substrate (*25*−*28*), and the developing negative charge at the carbonyl carbon is stabilized by hydrogen bonding to the neutral imidazole side chain of His-95 (*29*−*31*). The isomerization reaction is completed by reprotonation of the enediol(ate) intermediate at the adjacent carbon (Scheme 1).

We have shown that a large fraction (ca. 80%) of the enzymatic rate acceleration for the isomerization of GAP

[†] This work was supported by Grant GM 39754 from the National Institutes of Health. J.P.R. thanks the Science Foundation of Ireland for a Walton Fellowship, during which time this manuscript was prepared.

* To whom correspondence should be addressed. Tel: (716) 645 6800, ext 2194. Fax: (716) 645 6963. E-mail: jrichard@chem.buffalo.edu.

[1] Abbreviations: TIM, triosephosphate isomerase; GAP, (*R*)-glyceraldehyde 3-phosphate; DHAP, dihydroxyacetone phosphate; *d*-GAP, [2(*R*)-^{2}H]-glyceraldehyde 3-phosphate; *d*-DHAP, [1(*R*)-^{2}H]-dihydroxyacetone phosphate; D,L-GAP, D,L-glyceraldehyde 3-phosphate; NADH, nicotinamide adenine dinucleotide, reduced form; NMR, nuclear magnetic resonance.

10.1021/bi047954c CCC: $30.25
Published on Web 01/28/2005

catalyzed by TIM can be attributed to interactions between the enzyme and the remote nonreacting phosphodianion group of the substrate, which are utilized to stabilize the transition state for deprotonation of α-carbonyl carbon by 14 kcal/mol (*32*). It is clear that the tight binding of the transition state is the result of interactions of the substrate phosphodianion group with a "mobile loop" of ca. 10 amino acid residues (*10*, *17*, *33*−*37*) and with the positively charged Lys-12 in the active site (*38*, *39*). However, there is no consensus about the *physical* mechanism by which the interactions between TIM and the substrate phosphodianion group are "harnessed" to stabilize the transition state for proton transfer.

^{1}H NMR spectroscopy is a powerful analytical method for monitoring proton transfer from carbon in D_2O. It has been successfully used in determination of the carbon acidity of a variety of simple functional groups, including thiolesters (*40*), esters (*41*), amides (*42*), nitriles (*43*), and ketones (*44*), and in a study of enzymatic catalysis of the deprotonation of a thiolester (*45*). This technique provides very useful information about both the extent and the position of incorporation of deuterium into carbon acids. It is therefore very well suited for studies on the mechanism of action of TIM, because in D_2O the enediol(ate) intermediate should partition between reaction to form an aldehyde (GAP) and a ketone (DHAP) labeled with deuterium at the α-position.

We have shown in our earlier work that ^{1}H NMR spectroscopy can be used to monitor not only the velocity of turnover of the "unnatural" substrate (*R*)-glyceraldehyde by TIM in D_2O, but also the velocity of formation of the isomerization product dihydroxyacetone that proceeds with intramolecular transfer of hydrogen and with incorporation of deuterium from solvent at C-1, along with the velocity of formation of (*R*)-glyceraldehyde labeled with deuterium at C-2 (*32*). The success of these studies on (*R*)-glyceraldehyde prompted the work reported here on the TIM-catalyzed isomerization of the physiological substrate (*R*)-glyceraldehyde 3-phosphate (GAP) in D_2O. Our initial goal was to determine the effect of the phosphodianion group at GAP on the partitioning of the enediol(ate) intermediate in D_2O between formation of hydrogen- and deuterium-labeled products. However, the results of our experiments were entirely unexpected and have a broader significance than was envisioned at the outset of this work.

We report here that the TIM-catalyzed isomerization of GAP in D_2O gives a 49% yield of DHAP that forms by intramolecular transfer of hydrogen from substrate to product and smaller yields of [1(*R*)-^{2}H]-DHAP (*d*-DHAP) and [2(*R*)-^{2}H]-GAP (*d*-GAP) labeled with deuterium from solvent at C-1 and C-2, respectively. This stands in sharp contrast with the earlier observation that the reaction of tritium-labeled [1(*R*)-^{3}H]-DHAP in H_2O proceeds with up to only ca. 6% intramolecular transfer of the tritium label to the GAP product (*46*−*48*). Our results require a reevaluation of earlier conclusions about the dynamics of exchange of the hydron at the carboxylic acid side chain of Glu-165 at the TIM−enediol(ate) complex with those of bulk solvent.

MATERIALS AND METHODS

TIM from rabbit muscle (lyophilized powder) was purchased from Sigma and had a specific activity toward GAP of 5500−6000 units/mg at pH 7.5 and 25 °C. Glycerol 3-phosphate dehydrogenase from rabbit muscle (170 units/mg) was purchased from Boehringer. The plasmid pBSX1cTIM containing the wild-yype gene for TIM from chicken muscle (*49*) and *E. coli* strain DF502 (strep^R, tpi$^-$, and his$^-$) whose DNA lacks the gene for TIM (*50*) were generous gifts from Professor Nicole Sampson. *E. coli* DF502 was transformed with pBSX1cTIM, and triosephosphate isomerase was overexpressed and purified according to published procedures (*36*).[2] After passage down two DEAE-cellulose columns (Whatman DE52), the enzyme was judged to be homogeneous by gel electrophoresis and had a specific activity for turnover of GAP in 100 mM triethanolamine buffer at pH 7.5 of 6000 units/mg at 25 °C and 9000 units/mg at 30 °C (*51*).

Commercially available chemicals were reagent grade or better and were used without further purification. Deuterium oxide (99.9% D) and deuterium chloride (35% w/w, 99.9% D) were purchased from Cambridge Isotope Laboratories. Sodium deuterioxide (40 wt %, 99.9% D), triethanolamine hydrochloride, and tetramethylammonium hydrogensulfate were purchased from Aldrich. NADH (disodium salt), dihydroxyacetone phosphate (lithium salt), D,L-glyceraldehyde 3-phosphate diethyl acetal (barium salt), the dicyclohexylammonium salt of (*R*)-glyceraldehyde 3-phosphate diethyl acetal, and Dowex 50W (H^+ form, 100−200 mesh, 4% cross-linked) were purchased from Sigma. Imidazole was purchased from Fluka.

D,L-Glyceraldehyde 3-phosphate diethyl acetal was converted to the free aldehyde (D,L-GAP) by treatment with a suspension of Dowex 50W (H^+ form, 100−200 mesh, 4% cross-linked) in water at 90−100 °C for 5−10 min. The resulting aqueous solution of D,L-GAP (pH ∼2) was stored at −20 °C. Before use in routine enzyme assays the solution was adjusted to the appropriate pH by the addition of 1 M NaOH, after which it was stored at −20 °C. A similar procedure was used to prepare D,L-GAP in D_2O, except that the Dowex 50W was exchanged with several aliquots of D_2O before use.

Solutions of GAP in D_2O were prepared by passage of ca. 2 mL of a 50−80 mM solution of the dicyclohexylammonium salt of its diethyl acetal in D_2O down a short column of Dowex 50W that had been exchanged with D_2O. The free acid was eluted with D_2O, and the eluant (ca. 8 mL) was collected and its volume reduced to 1−2 mL by evaporation under reduced pressure. A 10−15 μL portion of 13 M DCl was added, and the hydrolysis of the diethyl acetal to give the free aldehyde at room temperature was monitored by ^{1}H NMR until it was ca. 99% complete, at which time ^{1}H NMR analysis showed that ≤2% of the product GAP had undergone conversion to methylglyoxal (*24*). The resulting solution of GAP in D_2O was stored at −20 °C and was adjusted to the appropriate pD immediately before use by the addition of 1 M NaOD.

Buffered solutions of imidazole in D_2O were prepared by dissolving neutral imidazole and NaCl in D_2O followed by addition of a measured amount of a stock solution of DCl to give the required acid/base ratio at $I = 0.1$ (NaCl).

[2] We are grateful to Professor Nicole Sampson for gifts of the plasmid pBSX1cTIM and *E. coli* strain DF502 and for expert help with the expression and purification of recombinant chicken muscle TIM.

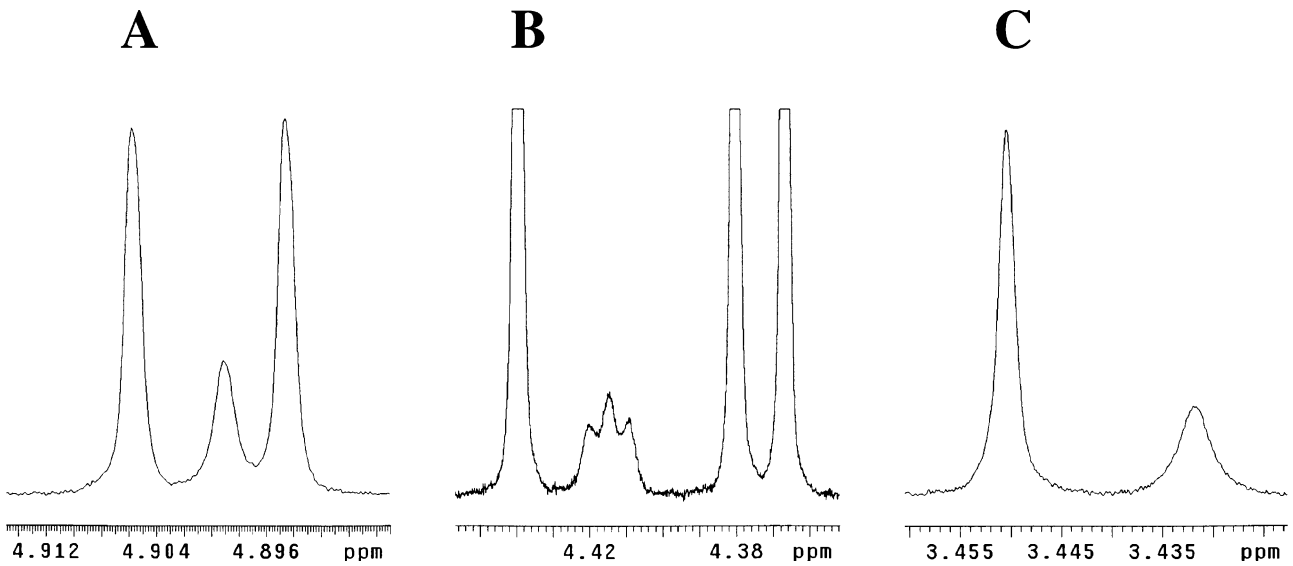

FIGURE 1: Representative partial ^{1}H NMR spectra of the remaining substrate and the triose phosphate products during the reaction of GAP (10 mM) catalyzed by rabbit muscle TIM (0.074 units/mL) in D_2O buffered by 21 mM imidazole at pD 7.9 and 25 °C ($I = 0.15$, NaCl). (A) The doublet ($J = 6$ Hz) at 4.900 ppm is due to the C-1 proton of GAP hydrate. The broad singlet at 4.899 ppm is due to the C-1 proton of [2(*R*)-^{2}H]-GAP hydrate. (B) The singlet at 4.440 ppm is due to the CH_2OD group of the keto form of DHAP. The upfield-shifted triplet ($J_{HD} = 2-3$ Hz) at 4.415 ppm is due to the CHDOD group of the keto form of [1(*R*)-^{2}H]-DHAP. The doublet ($J = 7$ Hz) at 4.374 ppm is due to the $CH_2OPO_3^{2-}$ group of the keto forms of both DHAP and [1(*R*)-^{2}H]-DHAP. (C) The singlet at 3.451 ppm is due to the CH_2OD group of DHAP hydrate. The upfield-shifted broad singlet at 3.432 ppm is due to the CHDOD group of [1(*R*)-^{2}H]-DHAP hydrate.

Buffered solutions of triethanolamine in H_2O or D_2O were prepared by a similar procedure by neutralization of triethanolamine hydrochloride with NaOH or NaOD. Solution pH or pD was determined at 25 °C using an Orion Model 720A pH meter equipped with a Radiometer pHC4006-9 combination electrode that was standardized at pH 7.00 and 10.00 at 25 °C. Values of pD were obtained by adding 0.40 to the observed reading of the pH meter (*52*).

Commercial rabbit muscle TIM was exhaustively dialyzed against 60 mM triethanolamine buffer (pD 7.5, $I = 0.1$, NaCl) in D_2O at 4 °C. Stock solutions of rabbit and recombinant chicken muscle TIMs were diluted 10 000-fold into 25 mM imidazole (pD 7.9, $I = 0.1$, NaCl) or 60 mM triethanolamine (pD 7.5, $I = 0.1$, NaCl) buffer in D_2O before use. Glycerol 3-phosphate dehydrogenase was exhaustively dialyzed against 20 mM triethanolamine buffer (pH 7.5) at 4 °C.

Enzyme Assays. All enzyme assays were carried out at 25 °C. Changes in the concentration of NADH were calculated using an extinction coefficient of 6220 M^{-1} cm^{-1} at 340 nm. One unit is the amount of enzyme that converts 1 μmol of substrate to product in 1 min under the specified conditions.

Glycerol 3-phosphate dehydrogenase was assayed by monitoring the enzyme-catalyzed oxidation of NADH by DHAP at 340 nm. The assay mixture contained 100 mM triethanolamine (pH 7.5, $I = 0.1$, NaCl), 0.2 mM NADH, and ca. 1 mM DHAP.

TIM was assayed by coupling the isomerization of GAP to the oxidation of NADH using glycerol 3-phosphate dehydrogenase (*53*), monitored at 340 nm. For routine assays the assay mixture contained 100 mM triethanolamine (pH 7.5, $I = 0.1$, NaCl), 0.2 mM NADH, ca. 6 mM D,L-GAP (3 mM GAP, $\sim 7K_m$ (*53*)), and 0.3 units of glycerol 3-phosphate dehydrogenase in a volume of 1 mL. The concentration of GAP in these assays and in the turnover of GAP by TIM in D_2O monitored by ^{1}H NMR was obtained from the change in absorbance at 340 nm upon its complete TIM-catalyzed conversion to DHAP that was coupled to the oxidation of NADH using glycerol 3-phosphate dehydrogenase.

A value of $K_m = 0.49$ mM was determined for the turnover of GAP by rabbit muscle TIM in 20 mM triethanolamine buffer at pD 7.9 and 25 °C ($I = 0.1$, NaCl).

^{1}H NMR Analyses. ^{1}H NMR spectra at 500 MHz were recorded in D_2O at 25 °C using a Varian Unity Inova 500 spectrometer that was shimmed to give a line width of ≤ 0.7 Hz for each peak of the doublet due to the C-1 proton of GAP hydrate. Spectra (16−64 transients) were obtained using a sweep width of 6000 Hz, a pulse angle of 90°, and an acquisition time of 7 s, with zero-filling of the data to 128 K. To ensure accurate integrals for the protons of interest, a relaxation delay between pulses of 127 s ($> 8T_1$) was used (see below). Baselines were subjected to a first-order drift correction before determination of integrated peak areas. Chemical shifts are reported relative to HOD at 4.67 ppm.

The following relaxation times T_1 were determined in D_2O at 25 °C: (a) the protons due to GAP hydrate (11 mM) in unbuffered solution at pD 7.9 ($I = 0.17$, NaCl), $T_1 = 2-5$ s; (b) the protons due to the free keto and hydrate forms of DHAP (33 mM) in unbuffered solution at pD 7.9 ($I = 0.1$, NaCl), $T_1 = 1-2$ s; (c) the protons due to methylglyoxal monohydrate (10 mM) in 48 mM imidazole buffer at pD 7.5 ($I = 0.1$, NaCl), $T_1 = 6-14$ s; (d) the C-4,5 protons of imidazole (25 mM) at pD 7.9 ($I = 0.1$, NaCl), $T_1 = 11$ s.

Baseline separation was obtained for almost all of the signals due to GAP hydrate and the products of the reactions of GAP in D_2O in the presence of TIM. The exception was the doublet ($J = 6$ Hz) at 4.900 ppm due to the C-1 proton of GAP hydrate and the broad singlet at 4.899 ppm due to the same proton at the hydrate of [2(*R*)-^{2}H]-GAP (*d*-GAP), which lies 0.001 ppm upfield from the midpoint of the two peaks of the doublet due to GAP hydrate (Figure 1A). Therefore, the integrated area of the doublet due to the C-1 proton of GAP hydrate was determined by multiplying the area of only the most downfield peak of the doublet by 2.

The area of the singlet due to the C-1 proton of *d*-GAP hydrate was then determined as the difference between the combined integrated areas of *all* the signals due to the C-1 protons of GAP hydrate and *d*-GAP hydrate and that calculated for the doublet due to GAP hydrate. Identical results were obtained when the integrated area of the singlet was obtained directly using the minima in the valleys between the peaks as the cutoffs for the integral.

Hydration of the Carbonyl Groups of Reactant and Products. The carbonyl groups of GAP, DHAP, and methylglyoxal are extensively hydrated in D_2O. A value of $f_{hyd} = 0.40$ for the fraction of DHAP present as the C-2 hydrate in 21 mM imidazole buffer in D_2O at pD 7.9 and 25 °C ($I = 0.15$, NaCl) was determined by ^{1}H NMR from the integrated areas of the singlets due to the C-1 protons of DHAP hydrate at 3.45 ppm and free DHAP at 4.44 ppm. This is similar to $f_{hyd} = 0.45$ in D_2O at pD 7 and 25 °C determined in an earlier study (*54*). A value of $f_{hyd} = 0.95$ for the fraction of GAP present as the C-1 hydrate in unbuffered D_2O at pD 7.9 and 25 °C ($I = 0.1$, NaCl) was determined by ^{1}H NMR from the integrated areas of the doublet due to the C-1 proton of GAP hydrate at 4.90 ppm and the triplet due to the C-2 proton of free GAP at 4.38 ppm. This is in good agreement with $f_{hyd} \approx 0.96$ in D_2O at neutral pD determined in an earlier study (*55*). Methylglyoxal exists as a mixture of the C-1 monohydrate and the C-1,C-2 bishydrate in aqueous solution (*56*). A value of $f_{monohyd} = 0.60$ for the fraction of methylglyoxal present as the C-1 monohydrate in 48 mM imidazole buffer in D_2O at pD 7.5 and 25 °C ($I = 0.1$, NaCl) was determined by ^{1}H NMR from the integrated areas of the singlets due to the C-3 protons of the monohydrate at 2.18 ppm and the bishydrate at 1.27 ppm.

TIM-Catalyzed Isomerization of GAP in D_2O Monitored by ^{1}H NMR. The turnover of GAP (10−12 mM, $\geq 20K_m$) by rabbit or chicken muscle TIM in 21−84 mM imidazole (pD 7.9) or 48 mM triethanolamine (pD 7.5) buffer in D_2O at 25 °C and $I = 0.15$ (NaCl) was followed by ^{1}H NMR spectroscopy. For experiments with chicken muscle TIM the reaction mixture also contained 2 mM tetramethylammonium hydrogensulfate as an internal standard.

Prior to the addition of enzyme, the ^{1}H NMR spectrum of the reaction mixture at "zero" reaction time was recorded using one of the following two procedures. (1) In the experiment with chicken muscle TIM, identical 750 μL aliquots of the reaction mixture containing buffer and substrate GAP were placed in two separate NMR tubes. In one tube the enzyme-catalyzed reaction was initiated by the addition of 10 μL of TIM in buffered D_2O, and the tube was incubated at 25 °C. Meanwhile, the ^{1}H NMR spectrum of the reaction mixture in the absence of TIM was recorded using the aliquot in the other tube. The progress of the reaction of GAP in the presence of TIM was then monitored by ^{1}H NMR spectroscopy at 25 °C. (2) For the experiments with rabbit muscle TIM, 750 μL of the reaction mixture containing buffer and substrate GAP was placed in an NMR tube and the ^{1}H NMR spectrum was recorded at 25 °C. This was immediately followed by the addition of 10 μL of TIM in buffered D_2O, and the progress of the reaction was then monitored by ^{1}H NMR spectroscopy at 25 °C. Each NMR spectrum was recorded over a period of 30−60 min, and the reaction time t was calculated from the time at the midpoint of these analyses.

The observed peak areas A_{obs} for the reactant GAP and the products *d*-GAP, DHAP, *d*-DHAP, and methylglyoxal determined by integration of ^{1}H NMR spectra obtained at various reaction times were normalized according to eq 1 to give A_P, where A_{std} and $(A_{std})_0$ are the observed peak areas of the signal due to the internal standard at time t and at $t = 0$, respectively. For experiments with rabbit muscle TIM the

$$A_P = A_{obs}\left(\frac{(A_{std})_0}{A_{std}}\right) \quad (1)$$

$$A_H = (A_{GAP})_0/0.95 \quad (2)$$

$$f_{GAP} = \frac{A_{GAP}/0.95}{A_H} \quad (3)$$

$$f_{d-GAP} = \frac{A_{d-GAP}/0.95}{A_H} \quad (4)$$

$$f_{DHAP} = \frac{A_{DHAP}/2}{A_H} \quad (5)$$

$$f_{d-DHAP} = \frac{A_{d-DHAP}}{A_H} \quad (6)$$

$$f_{MG} = \frac{\{A_{MG} - (A_{MG})_0\}/0.60}{A_H} \quad (7)$$

internal standard was either the singlet at 7.13 ppm due to the C-4,5 protons of the imidazole buffer or the triplet at 1.07 ppm due to the methyl group of ethanol that was present as a byproduct of the hydrolysis of GAP diethyl acetal. For experiments with chicken muscle TIM the internal standard was the signal at 3.08 ppm due to the methyl groups of added tetramethylammonium hydrogensulfate.

The disappearance of GAP was followed by monitoring the decrease in the normalized area A_{GAP} of the doublet ($J = 6$ Hz) at 4.900 ppm due to the C-1 proton of GAP hydrate, calculated using eq 1. The fraction of GAP remaining at time t was calculated using eq 3, where 0.95 is the fraction of GAP present as the C-1 hydrate and A_H is the normalized peak area for a *single* proton of *total* GAP at $t = 0$, calculated using eq 2.

The formation *d*-GAP was followed by monitoring the appearance of the singlet at 4.899 ppm due to the C-1 proton of *d*-GAP hydrate. This singlet is shifted slightly upfield (0.001 ppm) from the midpoint of the doublet at 4.900 ppm due to the C-1 proton of GAP hydrate, as a result of the presence of deuterium at C-2. The fraction of GAP converted to *d*-GAP was calculated using eq 4, where A_{d-GAP} is the normalized area of the singlet due to the C-1 proton of *d*-GAP hydrate calculated using eq 1, and 0.95 is the fraction of *d*-GAP present as the C-1 hydrate.

The formation of DHAP was followed by monitoring the appearance of the singlets at 3.451 and 4.440 ppm due to the two protons of the CH_2OD groups of the hydrate and keto forms of DHAP, respectively. The formation of *d*-DHAP was followed by monitoring the appearance of the

Scheme 2

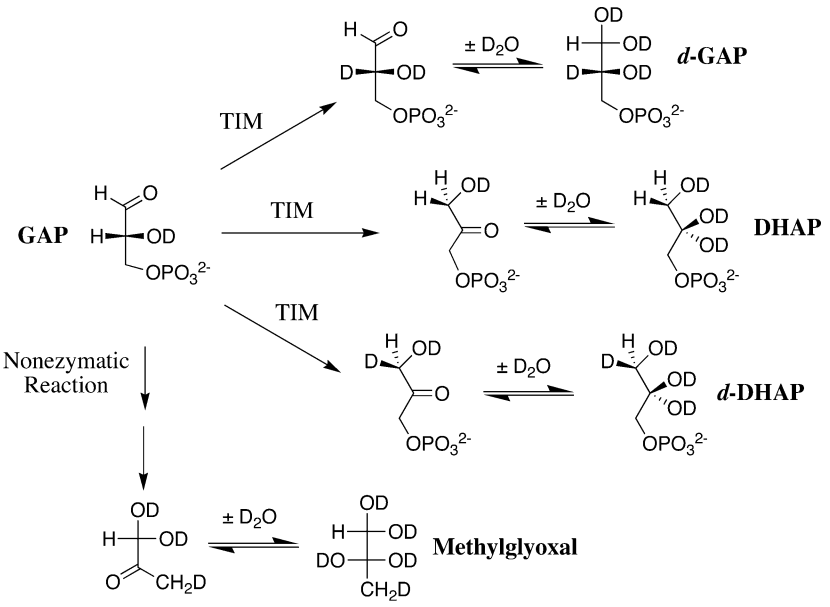

broad singlet at 3.432 ppm and the triplet (J_{HD} = 2−3 Hz) at 4.415 ppm due to the single proton of the CHDOD groups of the hydrate and keto forms of *d*-DHAP, respectively. The fraction of GAP converted to DHAP or *d*-DHAP was calculated from the *sum* of the normalized peak areas of the signals due to a *single* proton of the hydrate and keto forms of these products, $A_{DHAP}/2$ and A_{d-DHAP}, according to eqs 5 and 6. For the experiment in the presence of triethanolamine buffer, the signals due to the buffer obscured those due to the hydrates of DHAP and *d*-DHAP. In this case, the fraction of GAP converted to DHAP or *d*-DHAP was calculated from the normalized peak areas of the signals due to a single proton of only the keto forms of these products, with a correction for presence of 40% hydrate.

The formation of methylglyoxal was followed by monitoring the singlet at 5.17 ppm due to the C-1 proton of the monohydrate. The fraction of GAP converted to methylglyoxal was calculated from the *increase* in the normalized area of this singlet, $A_{MG} - (A_{MG})_0$, using eq 7, where 0.60 is the fraction of methylglyoxal present as the C-1 monohydrate.

RESULTS

The products of the TIM-catalyzed and nonenzymatic reactions of (*R*)-glyceraldehyde 3-phosphate (GAP) in D_2O are shown in Scheme 2. The disappearance of GAP and the appearance of the various reaction products in the presence of rabbit and chicken muscle TIM in D_2O at pD 7.5−7.9 and 25 °C were monitored by ^{1}H NMR spectroscopy.

Figure 1 shows representative partial ^{1}H NMR spectra of the remaining substrate and the triose phosphate products during the reaction of GAP (10 mM) catalyzed by rabbit muscle TIM in D_2O buffered with 21 mM imidazole at pD 7.9 and 25 °C (I = 0.15, NaCl). Figure 1A shows the doublet (J = 6 Hz) at 4.900 ppm due to the C-1 proton of GAP hydrate and the singlet at 4.899 ppm due to the C-1 proton of the hydrate of [2(*R*)-^{2}H]-GAP (*d*-GAP) labeled with deuterium at C-2. Figure 1B shows the singlet at 4.440 ppm due to the CH_2OD group of the keto form of dihydroxyacetone phosphate (DHAP), the upfield-shifted triplet (J_{HD} = 2−3 Hz) at 4.415 ppm due to the CHDOD group of the keto form of [1(*R*)-^{2}H]-DHAP (*d*-DHAP) labeled with deuterium at C-1, and the doublet (J = 7 Hz) at 4.374 ppm due to the $CH_2OPO_3^{2-}$ group of the keto forms of both DHAP and *d*-DHAP. Figure 1C shows the singlet at 3.451 ppm due to the CH_2OD group of DHAP hydrate and the broad upfield-shifted singlet at 3.432 ppm due to the CHDOD group of *d*-DHAP hydrate labeled with deuterium at C-1. The latter signal is in fact a barely resolved triplet with a very small (J < 1 Hz) H−D geminal coupling. However, we have found that it is not always possible to resolve the triplet due to the proton of a CHD group (*57*). The spectra in Figure 1 show that the incorporation of a single deuterium at the CH_2OD group of DHAP results in an isotope effect on the chemical shift of the remaining proton and upfield shifts of 0.025 and 0.019 ppm for the signals due to the keto and hydrate forms, respectively. These isotope shifts lie within the range of those we have observed for other deuterium-labeled methyl and methylene groups (*40*−*43*, *57*−*60*).

Figure 2 shows the change in the relative areas of the signals due to the C-1 proton(s) of the hydrates of the reactant GAP and the products *d*-GAP, DHAP, and *d*-DHAP during the reaction of GAP (10 mM) catalyzed by rabbit muscle TIM in D_2O buffered by 21 mM imidazole at pD 7.9 and 25 °C (I = 0.15, NaCl). The formation of methylglyoxal in the competing nonenzymatic elimination reaction of GAP (*24*) was followed by monitoring the singlet at 5.17 ppm due to the C-1 proton of methylglyoxal monohydrate (not shown). Methylglyoxal is the only significant product of the nonenzymatic reaction of GAP because, in the presence of low concentrations of buffer at neutral pH, the enediolate phosphate formed by deprotonation of GAP or DHAP undergoes elimination of phosphate ca. 100-fold faster than protonation at carbon (*24*). This was further confirmed in this work by ^{1}H NMR analysis of the reaction of D,L-GAP (11 mM) in 24 mM imidazole buffer in D_2O at pD 7.9 and 25 °C. Under these conditions there was no detectable (<1%) formation of DHAP during the reaction of up to 80% of the starting D,L-GAP.

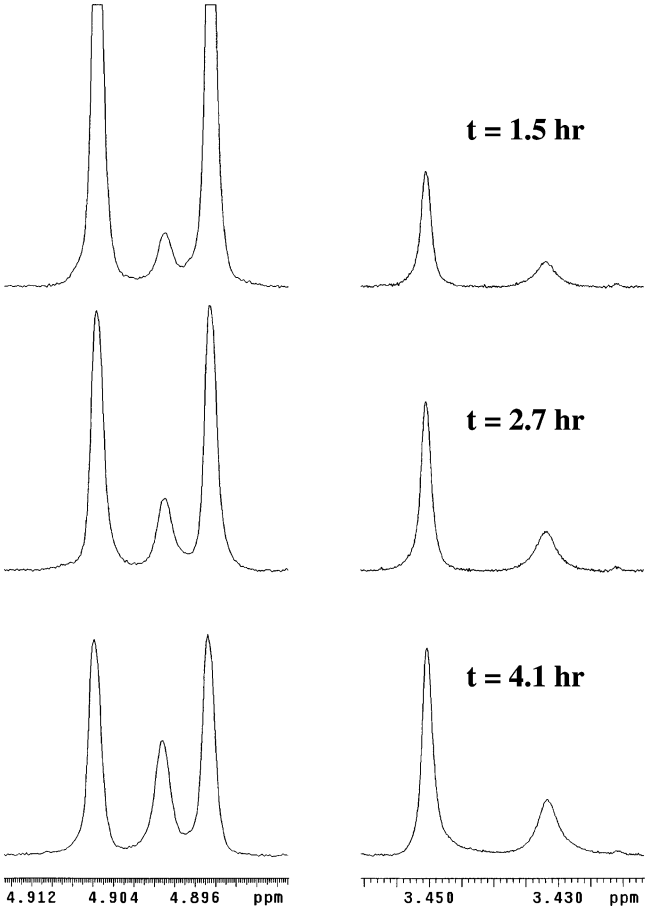

FIGURE 2: Change with time in the relative areas of the ^{1}H NMR signals due to the C-1 protons of the hydrates of the reactant and the products during the reaction of GAP (10 mM) catalyzed by rabbit muscle TIM (0.074 units/mL) in D_2O buffered by 21 mM imidazole at pD 7.9 and 25 °C (I = 0.15, NaCl). The disappearance of the doublet at 4.900 ppm due to the C-1 proton of GAP hydrate is accompanied by the appearance of singlets at 4.899, 3.451, and 3.432 ppm due to the C-1 protons of the products [2(*R*)-^{2}H]-GAP hydrate, DHAP hydrate, and [1(*R*)-^{2}H]-DHAP hydrate, respectively.

The fraction of substrate GAP remaining (eq 3) and the fractional formation of the products (eqs 4−7) of the TIM-catalyzed and spontaneous reactions of GAP at various reaction times were determined from the ratio of the normalized integrated area of the relevant signals due to the reactant or product (eq 1) and of the signal due to a *single* proton of *total* GAP at t = 0 (A_H, eq 2), as described in Materials and Methods. The sum of the observed fractions of GAP, *d*-GAP, DHAP, *d*-DHAP, and methylglyoxal decreased by less than 10% during the reaction of up to 80% of the starting GAP, which shows that all of the significant reaction products were identified by ^{1}H NMR. The formation of the triose phosphate products from the enzymatic reaction of GAP was accompanied by the formation of 9−42% methylglyoxal (Table 1) from the background nonenzymatic reaction. The large yield of 42% methylglyoxal observed for the reaction in the presence of 48 mM triethanolamine buffer at pD 7.5 reflects the greater reactivity of triethanolamine as compared to that of imidazole as a base catalyst of the nonenzymatic elimination reaction of GAP (*24*).

Figure 3A shows the decrease with time in the fraction of remaining GAP during the reaction of GAP (10 mM) catalyzed by chicken muscle TIM in D_2O buffered by 84 mM imidazole at pD 7.9 and 25 °C (I = 0.15, NaCl). Figure 3B shows the change in the fractional yields of *only* the triose phosphate products that arise from the enzymatic reaction of GAP in this experiment, $(f_P)_E$, which were normalized using the sum of the observed fractions of *d*-GAP, DHAP and *d*-DHAP according to eqs 8−10. There is no significant

$$(f_{d-\mathrm{GAP}})_E = \frac{f_{d-\mathrm{GAP}}}{f_{d-\mathrm{GAP}} + f_{\mathrm{DHAP}} + f_{d-\mathrm{DHAP}}} \quad (8)$$

$$(f_{\mathrm{DHAP}})_E = \frac{f_{\mathrm{DHAP}}}{f_{d-\mathrm{GAP}} + f_{\mathrm{DHAP}} + f_{d-\mathrm{DHAP}}} \quad (9)$$

$$(f_{d-\mathrm{DHAP}})_E = \frac{f_{d-\mathrm{DHAP}}}{f_{d-\mathrm{GAP}} + f_{\mathrm{DHAP}} + f_{d-\mathrm{DHAP}}} \quad (10)$$

change in the fractional yield of DHAP with time (Figure 3B, □), so that DHAP does not undergo significant TIM-catalyzed deuterium exchange during the reaction of GAP. The observed increase in the fractional yield of *d*-DHAP (Figure 3B, ■) and decrease in the fractional yield of *d*-GAP (Figure 3B, ●) with time is a result of TIM-catalyzed isomerization of *d*-GAP to give the thermodynamically favored product *d*-DHAP.

Table 1 gives the initial fractional yields of the triose phosphate products of the TIM-catalyzed reactions of GAP, f_E, determined by making a short extrapolation of the normalized product yields $(f_P)_E$ to zero reaction time (Figure 3B).

DISCUSSION

A single NMR analysis provides the relative concentrations of the remaining reactant GAP and the four products of its enzymatic and nonenzymatic reactions in D_2O (Scheme 2 and Table 1). These analyses are straightforward, direct, and highly reproducible, with the major source of error being the ca. 5% uncertainty in the integrated NMR peak areas. They are simpler and faster, and they provide a more complete set of product data, than the analyses used in earlier studies of TIM employing tritium at tracer levels as the second hydrogen isotope. For example, the earlier studies required in some cases the synthesis of tritium-labeled substrate and in all cases separation of the ^{3}H-labeled reactant, products, and solvent prior to determination of the tritium enrichment of the product and/or remaining reactant (*46*−*48*).

^{1}H NMR spectroscopy is a less sensitive method for monitoring hydron transfer than the radiochemical analyses that monitor the fate of a tritium label at substrate or solvent. For example, our work employed an initial concentration of substrate GAP (10−12 mM) that is far in excess of K_m = 0.49 mM determined for its TIM-catalyzed reaction in D_2O at pD 7.9 (see Materials and Methods). This is significant, because it was found that the fraction of the TIM-catalyzed reaction of [1(*R*)-^{3}H]-DHAP that proceeds with intramolecular transfer of the tritium label from substrate to product GAP in H_2O, determined after 50% reaction, increases from 1.2% for reactions conducted at low initial substrate concentrations (0.03−0.3 mM, 0.013−0.13 K_m) to 2.2% at intermediate concentrations (0.3−1.0 mM, 0.13−0.43 K_m) and then falls to 1.7% at high concentrations (1.0−7.0 mM, 0.43−3 K_m) (*48*).

Table 1: Product Distributions for the Reaction of (*R*)-Glyceraldehyde 3-Phosphate Catalyzed by Triosephosphate Isomerase in D_2O[a]

TIM (amt (units/mL))[c]	buffer system		fractional yield of product[b] DHAP	*d*-DHAP	*d*-GAP	methylglyoxal
chicken (0.038)	84 mM imidazole	f_T [d]	0.34	0.21	0.13	0.20
	pD 7.9	f_E [e]	0.50	0.31	0.19	
rabbit (0.038)	83 mM imidazole	f_T [d]	0.34	0.21	0.14	0.24
	pD 7.9	f_E [e]	0.49	0.31	0.20	
rabbit (0.074)	21 mM imidazole	f_T [d]	0.34	0.22	0.14	0.09
	pD 7.9	f_E [e]	0.48	0.32	0.20	
rabbit (0.031)	48 mM triethanolamine	f_T [d]	0.28	0.17	0.15	0.42
	pD 7.5	f_E [e]	0.47	0.28	0.25	
av		f_E [f]	0.49 ± 0.01	0.31 ± 0.02	0.21 ± 0.03	

$k_{ex}/(k_{C-1})_H = 1.04$;[g] $(k_{C-1})_D/(k_{C-2})_D = 1.48$[h]

[a] For reactions at 25 °C and $I = 0.15$ (NaCl). [b] Product yields were determined by ^{1}H NMR spectroscopy. [c] Activity for isomerization of GAP in H_2O at pH 7.5 and 25 °C. [d] Yields of the products of both the enzymatic and nonenzymatic reactions of GAP, determined by extrapolation of the values of $f_P/(1 - f_{GAP})$ to zero time, where f_P is the observed fraction of the product (eqs 4−7) and $1 - f_{GAP}$ is the fraction of GAP that has undergone reaction. [e] Yields of the products of *only* the enzymatic reaction GAP, determined by extrapolation of the normalized yields $(f_P)_E$ (eqs 8−10) to zero time (Figure 3B). [f] Average value of f_E for the reactions catalyzed by rabbit and chicken muscle TIM in the presence of the various buffers at pD 7.9 and 7.5. [g] Rate constant ratio for partitioning of the TIM−enediol(ate) complex labeled with hydrogen at Glu-165 between hydron exchange with solvent D_2O and intramolecular transfer of the substrate-derived hydrogen to product DHAP. [h] Rate constant ratio for partitioning of the TIM−enediol(ate) complex labeled with deuterium at Glu-165 between deuterium transfer to C-1 to give *d*-DHAP and to C-2 to give *d*-GAP.

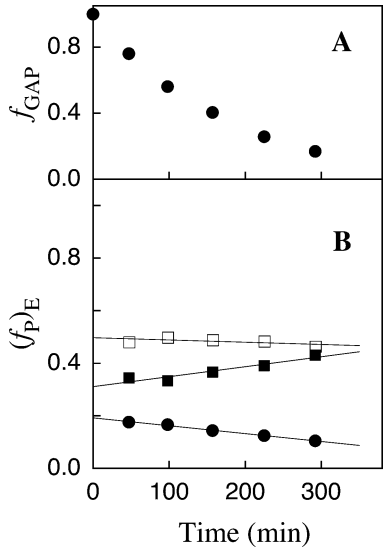

FIGURE 3: Product data for the reaction of GAP (10 mM) catalyzed by chicken muscle TIM (0.038 units/mL) in D_2O buffered by 84 mM imidazole at pD 7.9 and 25 °C ($I = 0.15$, NaCl), determined by ^{1}H NMR spectroscopy. (A) The decrease with time in the fraction of remaining GAP, calculated using eq 3. (B) The change with time in the fractional yields of only the triose phosphate products of the enzymatic reaction of GAP, normalized using the sum of the observed fractions of [2(*R*)-^{2}H]-GAP, DHAP, and [1(*R*)-^{2}H]-DHAP according to eqs 8−10. Short extrapolations of these data to zero time (solid lines) gave the initial product yields of the enzymatic reaction of GAP, f_E, reported in Table 1. Key: (□) yield of DHAP; (■) yield of [1(*R*)-^{2}H]-DHAP; (●) yield of [2(*R*)-^{2}H]-GAP.

"Simple" Comparisons with Earlier Work. This is the first report of the product distribution for the thermodynamically favorable ($K_{eq} = 22$) (*61*) TIM-catalyzed isomerization of GAP in D_2O. On the whole, the results of our experiments can be rationalized within the framework of the free energy profile developed by Knowles and co-workers in the classic studies of TIM that used tracer levels of tritium at substrate or solvent water (*2, 46, 62−65*). However, our results are very surprising in one respect (see below).

Scheme 3

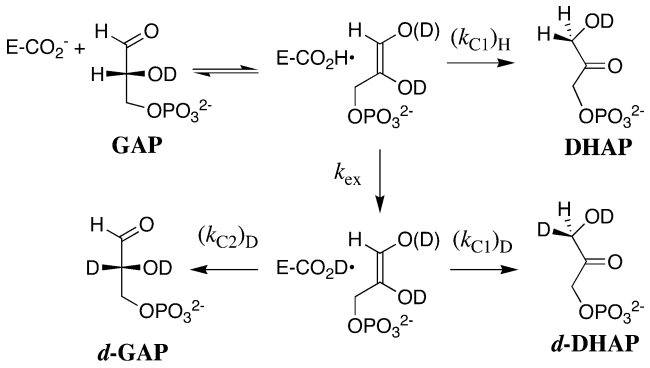

(a) Partitioning of the TIM−Enediol(ate) Intermediate between Hydron Exchange with Solvent D_2O and Intramolecular Transfer of ^{1}H Label from Substrate to Product. A value of $k_{ex}/(k_{C-1})_H = 1.04$ for partitioning of the TIM−enediol(ate) complex labeled at Glu-165 with ^{1}H derived from substrate GAP between hydron exchange with solvent D_2O (k_{ex}, Scheme 3) and intramolecular transfer of the ^{1}H label to product DHAP ($(k_{C-1})_H$, Scheme 3) can be calculated from the observed 49% yield of DHAP (Table 1). This result is startling, because it was shown in earlier studies of the TIM-catalyzed reaction of [1(*R*)-^{3}H]-DHAP labeled with tritium at tracer levels that the specific radioactivity of the product GAP at ca. 50% reaction is only 2−3% that of the starting DHAP and increases to only 6% after complete reaction of the substrate (*46−48*). The lower specific radioactivity of the product at early reaction times is due to discrimination against the reaction of [1(*R*)-^{3}H]-DHAP, as a result of a primary kinetic isotope effect (*2, 66*), and there is a corresponding increase in the tritium enrichment of substrate with time. The 6% intramolecular transfer of tritium from substrate DHAP to product GAP in H_2O (*46*) is substantially smaller than the 49% intramolecular transfer of hydrogen from substrate GAP to product DHAP in D_2O observed here.

Part or all of the difference in the extent of intramolecular transfer of the substrate-derived hydron observed for the

TIM-catalyzed reactions of GAP in D_2O and of [1(*R*)-^{3}H]-DHAP in H_2O is directly related to the use of a different substrate in these two sets of experiments. It was shown earlier, and confirmed here (see below), that reaction of the intermediate to form DHAP is ca. 3-fold faster than its reaction to form GAP (*64*). Therefore, there should be a ca. 3-fold increase in the ability of hydron exchange at the intermediate to compete with intramolecular transfer of the ^{1}H label when the formation of GAP from DHAP is monitored in D_2O than when the reverse formation of DHAP from GAP is monitored in this solvent. This prediction is confirmed in the following paper in this issue, which reports a smaller 18% intramolecular transfer of ^{1}H to product GAP during the isomerization of DHAP catalyzed by TIM in D_2O (*67*).

Along with a different substrate, these two sets of experiments also use a different isotopic label at both substrate (tritium or hydrogen) and solvent (H_2O or D_2O). The effect of these differences on partitioning of the intermediate between hydron exchange with solvent and intramolecular transfer of the substrate-derived hydron are considered in the following paper in this issue (*67*).

(b) Partitioning of the TIM−Enediol(ate) Intermediate between Formation of d-DHAP and d-GAP. A value of $(k_{C-1})_D/(k_{C-2})_D = 1.48$ for partitioning of the TIM−enediol(ate) intermediate labeled at Glu-165 with deuterium from solvent D_2O between hydron transfer to C-1 to form *d*-DHAP and to C-2 to form *d*-GAP (Scheme 3) can be calculated from the ratio of the yields of these two products from the reaction of GAP in D_2O (Table 1). This partitioning ratio is consistent with results from the earlier study of the TIM-catalyzed reaction of GAP in tritiated water, where it was shown that conversion of the reaction intermediate to product DHAP is ca. 3-fold faster than the formation of [2(*R*)-^{3}H]-GAP by incorporation of tritium from solvent at C-2 of the starting GAP (*64*). There is only a small 1.3-fold tritium discrimination isotope effect against the formation of [2(*R*)-^{3}H]-GAP (*63*), so that partitioning of the intermediate to form DHAP is ca. 3-fold faster than its partitioning to form GAP, with $(k_{C-1})_H/(k_{C-2})_H \approx 3$ for formation of ^{1}H-labeled DHAP and GAP from the intermediate. The somewhat smaller ratio of $(k_{C-1})_D/(k_{C-2})_D = 1.5$ for formation of *d*-DHAP and *d*-GAP in D_2O reported here can be attributed to the larger primary deuterium isotope effect on proton transfer to C-1 to form *d*-DHAP than on proton transfer to C-2 to form *d*-GAP (*2, 66*).

"Complex" Comparisons with Earlier Work. The following results from the breath-taking earlier work of Knowles and co-workers are consistent with the results reported here.

(1) The observation that the specific radioactivity of the product [1(*R*)-^{3}H]-DHAP formed by TIM-catalyzed isomerization of GAP in tritiated water is 13% of the specific radioactivity of the solvent is consistent with a 7.7-fold tritium discrimination isotope effect on protonation of the enediol(ate) intermediate to form [1(*R*)-^{3}H]-DHAP (*64*). By comparison, a significantly smaller primary tritium isotope effect of $(V/K)_T = 4.6$ for conversion of DHAP to the enediol(ate) intermediate can be calculated from the deuterium isotope effect of $(V/K)_D = 2.9$ determined for the isomerization of [1(*R*)-^{2}H]-DHAP (*66*), using the Swain−Schaad relationship $(V/K)_T = [(V/K)_D]^{1.44}$ (*68*). The ratio of these apparent tritium isotope effects for the reaction of DHAP to give the TIM−enediol(ate) intermediate in the forward and reverse directions, 4.6/7.7 = 0.60, is significantly smaller than the equilibrium isotope effect of around unity expected for deprotonation of DHAP (*69*).[3] In fact, these data are consistent with significant intramolecular transfer of ^{1}H from substrate GAP to give DHAP in ^3H_2O, because this will result in an *apparent* discrimination against the incorporation of tritium into the product DHAP that is unrelated to the intrinsic kinetic isotope effect on the proton-transfer step. For example, the observation that the specific radioactivity of the product DHAP is 13% that of the solvent is consistent with a smaller tritium discrimination isotope effect of ca. 4 and a reaction in which 51% of the TIM−enediol(ate) intermediate undergoes hydron exchange with bulk solvent, and 49% undergoes intramolecular transfer of the substrate-derived ^{1}H label to form DHAP, as is observed here in D_2O.

(2) The observation that there is no *detectable* primary deuterium isotope effect on k_{cat} for turnover of [2(*R*)-^{2}H]-GAP (*d*-GAP) by TIM in H_2O (*2, 66*) would appear to be inconsistent with a reaction in which there is significant intramolecular transfer of deuterium from *d*-GAP to give the product *d*-DHAP. This is because k_{cat} for the reaction of GAP is limited by proton transfer to the enediol(ate) to form DHAP (*2, 66*), so that if there were substantial intramolecular transfer of deuterium during the reaction of *d*-GAP in H_2O, then a primary deuterium isotope effect should be observed. However, the observed isotope effect of unity *can* be rationalized alongside the 49% intramolecular transfer of hydrogen for the reaction of GAP in D_2O observed here, because there should be a *smaller* fractional intramolecular transfer of deuterium during the reaction of *d*-GAP in H_2O. The equilibrium deuterium isotope effect on proton transfer from DHAP to give the TIM−enediol(ate) complex is expected to be around unity (see above), so that the primary deuterium isotope effect on proton transfer to the enediol(ate) to form DHAP is expected to be very similar to $(V/K)_D = 2.9$ determined for the turnover of *d*-DHAP (*66*) in the reverse direction. This should lead to a ca. 3-fold decrease in the partitioning of the enediol(ate) between intramolecular hydron transfer and hydron exchange with solvent for the reaction of *d*-GAP compared with GAP, reducing the fraction of *d*-GAP that reacts with intramolecular transfer of deuterium to ca. 24%. Therefore, 76% of the reaction of *d*-GAP in H_2O would proceed with hydron exchange to give DHAP with an isotope effect of unity, and 24% of the reaction would proceed with intramolecular transfer of deuterium to give *d*-DHAP with an isotope effect of ca. 3. The net effect would be a relatively small ca. 20% decrease in the reaction velocity, which would be difficult to detect.

Dynamics of Hydron Exchange at TIM. The observation of up to 6% intramolecular transfer of tritium from the substrate [1(*R*)-^{3}H]-DHAP to product GAP during TIM-catalyzed isomerization in H_2O (*46−48*) appears to be consistent with an enzyme active site and a bound enediol(ate) intermediate that is exposed to interaction with

[3] A value of ca. 1.0 is expected for the equilibrium tritium isotope effect on hydron transfer from the α-carbonyl carbon of bound substrate to the carboxylate anion side chain of Glu-165, because fractionation factors around unity have been reported for both α-carbonyl protons (Table 8 of ref 69) and carboxylic acid protons (Table 9 of ref 69).

Scheme 4

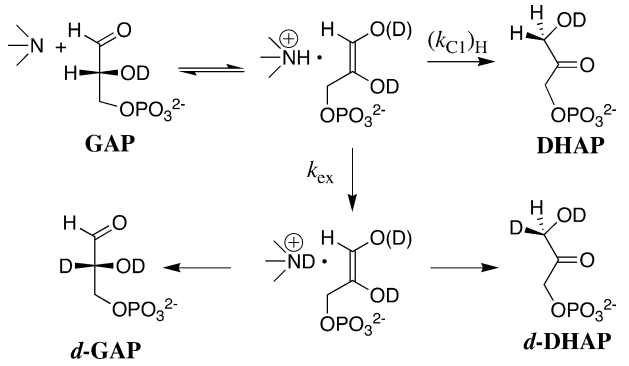

bulk solvent. This was implicit in the conclusion drawn in earlier studies that the substrate-derived hydron at the carboxylic acid side chain of Glu-165 in the TIM−enediol(ate) complex is "essentially at equilibrium" with those of bulk solvent (*2*). However, the results reported here require a revision of this conclusion, because a catalytic acid that partitions nearly equally between hydron exchange with solvent D_2O and proton transfer to the enediol(ate) to form DHAP ($k_{ex}/(k_{C-1})_H = 1.04$, Scheme 3 and Table 1) cannot be close to equilibrium with respect to hydron exchange with bulk solvent.

It is interesting to compare the partitioning of the enediol(ate) phosphate intermediate between hydron exchange and intramolecular transfer of a hydrogen label when the intermediate is formed in solution with its partitioning at the active site of TIM. The enediolate phosphate that forms by the nonenzymatic deprotonation of triose phosphates in water undergoes mainly elimination of phosphate to form, ultimately, methylglyoxal (*24*). However, the addition of buffer catalysts such as the tertiary amine 3-quinuclidinone ($pK_a = 7.5$) results in substantial Brønsted catalysis of proton transfer to the enediolate phosphate and an increase in the partitioning of this intermediate toward formation of the isomerization product (*24*). The deprotonation of GAP in water by 3-quinuclidinone (Scheme 4) gives an enediolate−3-quinuclidinone cation complex that is estimated to undergo irreversible diffusional separation to free ions with $k_{-d} = 1.6 \times 10^{10}$ s^{-1} (*70*), which is much faster than its collapse by proton transfer from the 3-quinuclidinone cation to C-1 to give DHAP with $(k_{C-1})_H \approx 7 \times 10^8$ s^{-1} (*24*). The diffusional separation of the complex in D_2O will result in the formation of products containing deuterium, so that $k_{ex} = k_{-d} = 1.6 \times 10^{10}$ s^{-1}. The resulting rate constant ratio $k_{ex}/(k_{C-1})_H \approx 23$ for partitioning of the intermediate leads to the expectation that the isomerization of GAP in D_2O catalyzed by 3-quinuclidinone will proceed with only ca. 4% intramolecular transfer of hydrogen to product DHAP (Scheme 4). This is much smaller than the 49% intramolecular transfer of hydrogen for the TIM-catalyzed isomerization of GAP in D_2O and corresponds to a ca. 20-fold *decrease* in $k_{ex}/(k_{C-1})_H$ for partitioning of the enediol(ate) between hydron exchange and proton transfer to C-1 upon binding to the isomerase.

The ca. 20-fold decrease in $k_{ex}/(k_{C-1})_H$ upon binding of the enediolate phosphate to TIM is consistent with an enzyme active site in which the catalytic acid/base is substantially shielded from hydron exchange with bulk solvent, because such shielding is expected to result in a decrease in k_{ex}. It is not easily accounted for by an increase in $(k_{C-1})_H$, because binding of the enediolate phosphate to TIM stabilizes the intermediate relative to reactant and thereby lowers the activation barrier to its formation (*24*, *71*). This stabilization is expected to result in a corresponding *decrease* in $(k_{C-1})_H$ for protonation of the intermediate (Schemes 3 and 4).

A simple strategy for enzymatic catalysis of proton transfer at carbon is to sequester the substrate at an active site with an effective dielectric constant that is lower than that of solvent water. For TIM, this will favor the rapid deprotonation of its carbon acid substrates by enhancing the Brønsted basicity of the carboxylate anion side chain of Glu-165 (*72*, *73*) and by strengthening stabilizing electrostatic and hydrogen-bonding interactions between the enzyme and the enediol(ate) intermediate and/or transition state for its formation, relative to the corresponding interactions in the polar solvent water (*74*−*76*). Our results provide strong evidence that the enediol(ate) phosphate intermediate is bound to TIM in an active site that is largely sequestered from bulk solvent. They are consistent with substantial shielding of the active site from bulk solvent, which will have the effect of reducing the effective dielectric constant of the active site to below that of water and toward the lower values estimated for the interiors of proteins (*77*−*81*). The following observations provide additional strong support for the conclusion that the TIM-catalyzed isomerization of triose phosphates occurs at an active site that is largely sequestered from solvent water.

(1) "Pulsing" by incubation of TIM in a small volume of highly radioactive tritiated water, followed by a large dilution into a "chase" solution of DHAP in unlabeled water, results in TIM-catalyzed formation of tritium-labeled DHAP and GAP (*82*). The total tritium incorporation into these triose phosphates shows saturation at high initial concentrations of DHAP in the chase and corresponds to a limiting value of 1−3 mol of tritium/mol of TIM, depending upon the source of TIM. No incorporation of tritium into DHAP or GAP is observed when DHAP is added 1−2 s after the "chase" with unlabeled water. These data provide strong evidence for a "pool" of hydrons at the binding pocket of TIM that remain bound long enough to allow for the binding of DHAP, its enzyme-catalyzed deprotonation, and reprotonation of the enediol(ate) intermediate to give tritium-labeled DHAP and GAP (*82*).

(2) The −NOH proton of the enediolate phosphate analogue phosphoglycolohydroxamic acid bound to yeast TIM exhibits a chemical shift of 14.9 ppm, which is deshielded by ca. 6.2 ppm from its value in DMSO (*83*). This proton also has an unusually small fractionation factor of $\phi = 0.38$ (*83*). These data provide evidence for the formation of a low-barrier hydrogen bond (*84*, *85*) at an enzyme active site of low effective dielectric constant that favors the formation of such hydrogen bonds (*75*, *76*).

(3) Binding of the enediolate phosphate analogue phosphoglycolohydroxamic acid to yeast TIM results in a 44-fold decrease in the rate constant for exchange of the NϵH proton of the active site residue His-95 with those of solvent water at 30 °C (*83*). This is consistent with shielding of His-95 at the TIM−enediol(ate) complex from its interaction with bulk solvent.

(4) TIM contains a "mobile loop" of ca. 10 highly conserved and largely hydrophobic residues (Pro-166−Ala-176) that serves as a "lid" for the active site (*17*, *33*−*36*).

These residues are thought to move as a rigid entity (*17*), and there is abundant evidence that substrate binding is accompanied by a large protein motion as the mobile loop moves to cover the phosphodianion group of the substrate and "close" the active site (*13*, *17*, *37*, *86*−*88*). This should at least partially sequester the bound substrate/intermediate from interaction with the bulk solvent.

(5) Comparison of the X-ray crystal structures determined for wild-yype yeast TIM and the K12M/G15A double mutant revealed that the Lys to Met mutation results in the inability of TIM to bind the enediolate phosphate analogue phophoglycolohydroxamic acid and provided evidence that this effect is electrostatic rather than steric in origin (*39*). The K12M mutation results in at least a 2×10^5-fold reduction in k_{cat}/K_m for isomerization of GAP, which corresponds to a >7 kcal/mol decrease in the stability of the transition state for isomerization (*38*). These observations are consistent with a low effective dielectric constant at the active site of TIM that favors a strong electrostatic interaction between the cationic side-chain of Lys-12 and the phosphodianion group of the substrate.

(6) The pH dependence of binding of the enediolate phosphate analogue phosphoglycolic acid (*21*, *89*, *90*) to rabbit muscle TIM is consistent with the titration of a group with an apparent pK_a of 6.5 (*91*). However, the demonstration that this inhibitor binds as its *trianion* rather than its dianion to a form of TIM that contains one more proton than does the free enzyme then implies p$K_a \approx 6.5$ for the carboxylate side chain of Glu-165 in the TIM−phosphoglycolate complex (*92*). This is substantially higher than p$K_a = 3.9$ estimated for Glu-165 at the free enzyme from the pH−rate profile for inactivation of yeast TIM by 3-chloroacetol sulfate (*91*). A simple explanation for this upward perturbation in the pK_a of the active site carboxylate side chain is that binding of the reaction intermediate is accompanied by a substantial decrease in the local dielectric constant of the enzyme active site.

(7) X-ray crystallographic and kinetic studies of the E165D and H95N mutants of chicken muscle TIM, and the E165D/S96P and H95N/S96P double mutants, showed that the enzymatic activity is surprisingly sensitive to variations in the presence and position of several ordered water molecules in the active site that occur when the hydroxymethyl group of serine is replaced by the relatively bulky side chain of proline (*93*−*95*). These effects are subtle and difficult to rationalize but are consistent with the notion that the catalytic efficiency of TIM stems from an active site that is highly organized and largely sequestered from bulk solvent.

REFERENCES

1. Rieder, S. V., and Rose, I. A. (1959) Mechanism of the triose phosphate isomerase reaction, *J. Biol. Chem. 234*, 1007−1010.
2. Knowles, J. R., and Albery, W. J. (1977) Perfection in Enzyme Catalysis: The Energetics of Triosephosphate Isomerase, *Acc. Chem. Res. 10*, 105−111.
3. Shonk, C. E., and Boxer, G. E. (1964) Enzyme Patterns in Human Tissues. I. Methods for the Determination of Glycolytic Enzymes, *Cancer Res. 24*, 709−721.
4. Gerlt, J. A., and Gassman, P. G. (1993) An Explanation for Rapid Enzyme-Catalyzed Proton Abstraction from Carbon Acids: Importance of Late Transition States in Concerted Mechanisms, *J. Am. Chem. Soc. 115*, 11552−11568.
5. Gerlt, J. A., and Gassman, P. G. (1993) Understanding the Rates of Certain Enzyme-Catalyzed Reactions: Proton Abstraction from Carbon Acids, Acyl-Transfer Reactions, and Displacement Reactions of Phosphodiesters, *Biochemistry 32*, 11943−11952.
6. Belasco, J. G., and Knowles, J. R. (1980) Direct Observation of Substrate Distortion by Triosephosphate Isomerase using Fourier Transform Infrared Spectroscopy, *Biochemistry 19*, 472−477.
7. Browne, C. A., Campbell, I. D., Kiener, P. A., Phillips, D. C., Waley, S. G., and Wilson, I. A. (1976) Studies of the histidine residues of triose phosphate isomerase by proton magnetic resonance and X-ray crystallography, *J. Mol. Biol. 100*, 319−343.
8. Webb, M. R., Standring, D. N., and Knowles, J. R. (1977) Phosphorus-31 Nuclear magnetic resonance of Dihydroxyacetone phosphate in the Presence of triosephosphate Isomerase. The Question of Nonproductive Binding of the Substrate Hydrate, *Biochemistry 16*, 2738−2741.
9. Tomita, Y., O'Connor, E. J., and McDermott, A. (1994) A Method for Dihedral Angle Measurement in Solids: Rotational Resonance NMR of a Transition-State Inhibitor of Triose Phosphate Isomerase, *J. Am. Chem. Soc. 116*, 8766−8771.
10. Williams, J. C., and McDermott, A. E. (1995) Dynamics of the Flexible Loop of Triose-Phosphate Isomerase: The Loop Motion Is Not Ligand Gated, *Biochemistry 34*, 8309−8319.
11. Banner, D. W., Bloomer, A. C., Petsko, G. A., Phillips, D. C., Pogson, C. I., Wilson, I. A., Corran, P. H., Furth, A. J., Milman, J. D., Offord, R. E., Priddle, J. D., and Waley, S. G. (1975) Structure of chicken muscle triose phosphate isomerase determined crystallographically at 2.5 Å resolution using amino acid sequence data, *Nature 255*, 609−614.
12. Lolis, E., Alber, T., Davenport, R. C., Rose, D., Hartman, F. C., and Petsko, G. A. (1990) Structure of Yeast Triosephosphate Isomerase at 1.9 Å Resolution, *Biochemistry 29*, 6609−6618.
13. Lolis, E., and Petsko, G. A. (1990) Crystallographic Analysis of the Complex between Triosephosphate Isomerase and 2-Phosphoglycolate at 2.5 Å Resolution: Implications for Catalysis, *Biochemistry 29*, 6619−6625.
14. Straus, D., Raines, R., Kawashima, E., Knowles, J. R., and Gilbert, W. (1985) Active site of triosephosphate isomerase: in vitro mutagenesis and characterization of an altered enzyme, *Proc. Natl. Acad. Sci. U.S.A. 82*, 2272−2276.
15. Blacklow, S. C., and Knowles, J. R. (1990) How Can a Catalytic Lesion be Offset? The Energetics of Two Pseudorevertant Triosephosphate Isomerases, *Biochemistry 29*, 4099−4108.
16. Alagona, G., Desmeules, P., Ghio, C., and Kollman, P. A. (1984) Quantum Mechanical and Molecular Mechanical Studies on a Model for the Dihydroxyacetone Phosphate-Glyceraldehyde Phosphate Isomerization Catalyzed by Triose Phosphate Isomerase (TIM), *J. Am. Chem. Soc. 106*, 3623−3632.
17. Joseph, D., Petsko, G. A., and Karplus, M. (1990) Anatomy of a conformational change: hinged "lid" motion of the triosephosphate isomerase loop, *Science 249*, 1425−1428.
18. Bash, P. A., Field, M. J., Davenport, R. C., Petsko, G. A., Ringe, D., and Karplus, M. (1991) Computer Simulation and Analysis of the Reaction Pathway of Triosephosphate Isomerase, *Biochemistry 30*, 5826−5832.
19. Alagona, G., Ghio, C., and Kollman, P. A. (1996) Chemical reaction mechanisms in vacuo, in solution and in enzyme fields: isomerization catalyzed by triose phosphate isomerase (TIM), *THEOCHEM 371*, 287−298.
20. Cui, Q., and Karplus, M. (2001) Triosephosphate Isomerase: A Theoretical Comparison of Alternative Pathways, *J. Am. Chem. Soc. 123*, 2284−2290.
21. Wolfenden, R. (1969) Transition State Analogues for Enzyme Catalysis, *Nature 223*, 704−705.
22. Collins, K. D. (1974) Activated intermediate analog. Use of phosphoglycolohydroxamate as a stable analog of a transiently occurring dihydroxyacetone phosphate-derived enolate in enzymic catalysis, *J. Biol. Chem. 249*, 136−142.
23. Albery, W. J., and Knowles, J. R. (1976) Evolution of Enzyme Function and the Development of Catalytic Efficiency, *Biochemistry 15*, 5631−5640.
24. Richard, J. P. (1984) Acid−Base Catalysis of the Elimination and Isomerization Reactions of Triose Phosphates, *J. Am. Chem. Soc. 106*, 4926−4936.
25. Waley, S. G., Miller, J. C., Rose, I. A., and O'Connell, E. L. (1970) Identification of site in triose phosphate isomerase labeled by glycidol phosphate, *Nature 227*, 181.
26. Coulson, A. F. W., Knowles, J. R., Priddle, J. D., and Offord, R. E. (1970) Uniquely labeled active site sequence in chicken muscle triose phosphate isomerase, *Nature 227*, 180−181.

27. Hartman, F. C. (1970) Isolation and Characterization of an Active-Site Peptide from Triose Phosphate Isomerase, *J. Am. Chem. Soc. 92*, 2170−2172.
28. Joseph-McCarthy, D., Rost, L. E., Komives, E. A., and Petsko, G. A. (1994) Crystal Structure of the Mutant Yeast Triosephosphate Isomerase in Which the Catalytic Base Glutamic Acid 165 Is Changed to Aspartic Acid, *Biochemistry 33*, 2824−2829.
29. Nickbarg, E. B., Davenport, R. C., Petsko, G. A., and Knowles, J. R. (1988) Triosephosphate Isomerase: Removal of a Putatively Electrophilic Histidine Residue Results in a Subtle Change in Catalytic Mechanism, *Biochemistry 27*, 5948−5960.
30. Komives, E. A., Chang, L. C., Lolis, E., Tilton, R. F., Petsko, G. A., and Knowles, J. R. (1991) Electrophilic Catalysis in Triosephosphate Isomerase: The Role of Histidine-95, *Biochemistry 30*, 3011−3019.
31. Lodi, P. J., and Knowles, J. R. (1991) Neutral Imidazole Is the Electrophile in the Reaction Catalyzed by Triosephosphate Isomerase: Structural Origins and Catalytic Implications, *Biochemistry 30*, 6948−6956.
32. Amyes, T. L., O'Donoghue, A. C., and Richard, J. P. (2001) Contribution of Phosphate Intrinsic Binding Energy to the Rate Acceleration of Triosephosphate Isomerase, *J. Am. Chem. Soc. 123*, 11325−11326.
33. Pompliano, D. L., Peyman, A., and Knowles, J. R. (1990) Stabilization of a Reaction Intermediate as a Catalytic Device: Definition of the Functional Role of the Flexible Loop in Triosephosphate Isomerase, *Biochemistry 29*, 3186−3194.
34. Sampson, N. S., and Knowles, J. R. (1992) Segmental Movement: Definition of the Structural Requirements for Loop Closure in Catalysis by Triosephosphate Isomerase, *Biochemistry 31*, 8482−8487.
35. Sampson, N. S., and Knowles, J. R. (1992) Segmental Motion in Catalysis: Investigation of a Hydrogen Bond Critical for Loop Closure in the Reaction of Triosephosphate Isomerase, *Biochemistry 31*, 8488−8494.
36. Sun, J., and Sampson, N. S. (1999) Understanding Protein Lids: Kinetic Analysis of Active Hinge Mutants in Triosephosphate Isomerase, *Biochemistry 38*, 11474−11481.
37. Rozovsky, S., Jogl, G., Tong, L., and McDermott, A. E. (2001) Solution-state NMR investigations of triosephosphate isomerase active site loop motion: Ligand release in relation to active site loop dynamics, *J. Mol. Biol. 310*, 271−280.
38. Lodi, P. J., Chang, L. C., Knowles, J. R., and Komives, E. A. (1994) Triosephosphate Isomerase Requires a Positively Charged Active Site: The Role of Lysine-12, *Biochemistry 33*, 2809−2814.
39. Joseph-McCarthy, D., Lolis, E., Komives, E. A., and Petsko, G. A. (1994) Crystal Structure of the K12M/G15A Triosephosphate Isomerase Double Mutant and Electrostatic Analysis of the Active Site, *Biochemistry 33*, 2815−2823.
40. Amyes, T. L., and Richard, J. P. (1992) Generation and Stability of a Simple Thiol Ester Enolate in Aqueous Solution, *J. Am. Chem. Soc. 114*, 10297−10302.
41. Amyes, T. L., and Richard, J. P. (1996) Determination of the pK_a of Ethyl Acetate: Brønsted Correlation for Deprotonation of a Simple Oxygen Ester in Aqueous Solution, *J. Am. Chem. Soc. 118*, 3129−3141.
42. Richard, J. P., Williams, G., O'Donoghue, A. C., and Amyes, T. L. (2002) Formation and Stability of Enolates of Acetamide and Acetate Anion: An Eigen Plot for Proton Transfer at α-Carbonyl Carbon, *J. Am. Chem. Soc. 124*, 2957−2968.
43. Richard, J. P., Williams, G., and Gao, J. (1999) Experimental and Computational Determination of the Effect of the Cyano Group on Carbon Acidity in Water, *J. Am. Chem. Soc. 121*, 715−726.
44. Chiang, Y., Griesbeck, A. G., Heckroth, H., Hellrung, B., Kresge, A. J., Meng, Q., O'Donoghue, A. C., Richard, J. P., and J. Wirz. (2001) Keto−Enol/Enolate Equilibria in the *N*-Acetylamino-*p*-methylacetophenone System. Effect of a *β*-Nitrogen Substituent, *J. Am. Chem. Soc. 124*, 8979−8984.
45. D'Ordine, R. L., Bahnson, B. J., Tonge, P. J., and Anderson, V. E. (1994) Enoyl-Coenzyme A Hydratase-Catalyzed Exchange of the α-Protons of Coenzyme A Thiol Esters: A Model for an Enolized Intermediate in the Enzyme-Catalyzed Elimination? *Biochemistry 33*, 14733−14741.
46. Herlihy, J. M., Maister, S. G., Albery, W. J., and Knowles, J. R. (1976) Energetics of Triosephosphate Isomerase: The Fate of the 1(*R*)-^{3}H Label of Tritiated Dihydroxyacetone Phosphate in the Isomerase Reaction, *Biochemistry 15*, 5601−5607.
47. Nickbarg, E. B., and Knowles, J. R. (1988) Triosephosphate Isomerase: Energetics of the Reaction Catalyzed by the Yeast Enzyme Expressed in *Escherichia coli*, *Biochemistry 27*, 5939−5947.
48. Harris, T. K., Cole, R. N., Comer, F. I., and Mildvan, A. S. (1998) Proton Transfer in the Mechanism of Triosephosphate Isomerase, *Biochemistry 37*, 16828−16838.
49. Hermes, J. D., Parekh, S. M., Blacklow, S. C., Koster, H., and Knowles, J. R. (1989) A reliable method for random mutagenesis: the generation of mutant libraries using spiked oligodeoxyribonucleotide primers, *Gene 84*, 143−151.
50. Straus, D., and Gilbert, W. (1985) Chicken triosephosphate isomerase complements an *Escherichia coli* deficiency, *Proc. Natl. Acad. Sci. U.S.A. 82*, 2014−2018.
51. Putman, S. J., Coulson, A. F. W., Farley, I. R. T., Riddleston, B., and Knowles, J. R. (1972) Specificity and kinetics of triose phosphate isomerase from chicken muscle, *Biochem. J. 129*, 301−310.
52. Glasoe, P. K., and Long, F. A. (1960) Use of Glass Electrodes To Measure Acidities in Deuterium Oxide, *J. Phys. Chem. 64*, 188−190.
53. Plaut, B., and Knowles, J. R. (1972) pH-Dependence of the triose phosphate isomerase reaction, *Biochem. J. 129*, 311−320.
54. Gray, G. R., and Barker, R. (1970) Studies on the Substrates of D-Fructose 1,6-Diphosphate Aldolase in Solution, *Biochemistry 9*, 2454−2562.
55. Trentham, D. R., McMurray, C. H., and Pogson, C. I. (1969) Active chemical state of D-glyceraldehyde-3-phosphate in its reactions with D-glyceraldehyde-3-phosphate dehydrogenase, aldolase, and triose phosphate isomerase, *Biochem. J. 114*, 19−24.
56. Guthrie, J. P., and Cossar, J. (1986) The pK_a values of simple aldehydes determined by kinetics of chlorination, *Can. J. Chem. 64*, 2470−2474.
57. Rios, A., Richard, J. P., and Amyes, T. L. (2002) Formation and Stability of Peptide Enolates in Aqueous Solution, *J. Am. Chem. Soc. 124*, 8251−8259.
58. Richard, J. P., and Nagorski, R. W. (1999) Mechanistic Imperatives for Catalysis of Aldol Addition Reactions: Partitioning of the Enolate Intermediate between Reaction with Brønsted Acids and the Carbonyl Group, *J. Am. Chem. Soc. 121*, 4763−4770.
59. Rios, A., Amyes, T. L., and Richard, J. P. (2000) Formation and Stability of Organic Zwitterions in Aqueous Solution: Enolates of the Amino Acid Glycine and Its Derivatives, *J. Am. Chem. Soc. 122*, 9373−9385.
60. Nagorski, R. W., and Richard, J. P. (2001) Mechanistic Imperatives for Aldose-Ketose Isomerization in Water: Specific, General Base- and Metal Ion-Catalyzed Isomerization of Glyceraldehyde with Proton and Hydride Transfer, *J. Am. Chem. Soc. 123*, 794−802.
61. Veech, R. L., Raijman, L., Dalziel, K., and Krebs, H. A. (1969) Disequilibrium in the triose phosphate isomerase system in rat liver, *Biochem. J. 115*, 837−842.
62. Albery, W. J., and Knowles, J. R. (1976) Deuterium and Tritium Exchange in Enzyme Kinetics, *Biochemistry 15*, 5588−5600.
63. Maister, S. G., Pett, C. P., Albery, W. J., and Knowles, J. R. (1976) Energetics of Triosephosphate Isomerase: The Appearance of Solvent Tritium in Substrate Dihydroxyacetone Phosphate and in Product, *Biochemistry 15*, 5607−5612.
64. Fletcher, S. J., Herlihy, J. M., Albery, W. J., and Knowles, J. R. (1976) Energetics of Triosephosphate Iisomerase: The Appearance of Solvent Tritium in Substrate Glyceraldehyde 3-Phosphate and in Product, *Biochemistry 15*, 5612−5617.
65. Albery, W. J., and Knowles, J. R. (1976) Free-Energy Profile for the Reaction Catalyzed by Triosephosphate Isomerase, *Biochemistry 15*, 5627−5631.
66. Leadlay, P. F., Albery, W. J., and Knowles, J. R. (1976) Energetics of Triosephosphate Isomerase: Deuterium Isotope Effects in the Enzyme-Catalyzed Reaction, *Biochemistry 15*, 5617−5620.
67. O'Donoghue, A. C., Amyes, T. L., and Richard, J. P. (2005) Hydron Transfer Catalyzed by Triosephosphate Isomerase. The Products of Isomerization of Dihydroxyacetone Phosphate in D_2O, *Biochemistry 44*, 2622−2631.
68. Swain, C. G., Stivers, E. C., Reuwer, J. F., and Schaad, L. J. (1958) The Swain-Schaad Relationship, *J. Am. Chem. Soc. 80*, 5885−5893.
69. Kresge, A. J., O'Ferrall, R. A. M., and Powell, M. F. (1987) Solvent Isotope Effects, Fractionation Factors and Mechanisms of Proton-Transfer Reactions, In *Isotopes in Organic Chemistry* (Buncel, E., and Lee, C. C., Eds.), Elsevier, New York.

70. Richard, J. P., and Jencks, W. P. (1984) Reactions of Substituted 1-Phenylethyl Carbocations with Alcohols and Other Nucleophilic Reagents, *J. Am. Chem. Soc. 106*, 1373−1383.
71. Richard, J. P. (1987) Isomerization Mechanisms through Hydrogen and Carbon Transfer, In *Enzyme Mechanisms* (Page, M. I., and Williams, A., Eds.), pp 298−316, Royal Society of Chemistry, London.
72. Kemp, D. S., and Paul, K. G. (1975) The Physical Organic Chemistry of Benzisoxazoles. III. The Mechanism and the Effects of Solvents on Rates of Decarboxylation of Benzisoxazole-3-carboxylic Acids, *J. Am. Chem. Soc. 97*, 7305−7312.
73. Gilbert, H. F. (1981) Proton Transfer from Acetyl-coenzyme A Catalyzed by Thiolase 1 from Porcine Heart, *Biochemistry 20*, 5643−5649.
74. King, G., Lee, F. S., and Warshel, A. (1991) Microscopic simulations of macroscopic dielectric constants of solvated proteins, *J. Chem. Phys. 95*, 4366−4377.
75. Scheiner, S., and Kar, T. (1995) The Nonexistence of Specially Stabilized Hydrogen Bonds in Enzymes, *J. Am. Chem. Soc. 117*, 6970−6975.
76. Pan, Y., and McAllister, M. A. (1997) Characterization of Low-Barrier Hydrogen Bonds. 1. Microsolvation Effects. An ab Initio and DFT Investigation, *J. Am. Chem. Soc. 119*, 7561−7566.
77. Sham, Y. Y., Muegge, I., and Warshel, A. (1998) The effect of protein relaxation on charge−charge interactions and dielectric constants of proteins, *Biophys. J. 74*, 1744−1753.
78. Simonson, T., and Brooks, C. L. (1996) Charge Screening and the Dielectric Constant of Proteins: Insights for Molecular Dynamics, *J. Am. Chem. Soc. 118*, 8452−8458.
79. Simonson, T., Carlsson, J., and Case, D. A. (2004) Proton Binding to Proteins: pK_a Calculations with Explicit and Implicit Solvent Models, *J. Am. Chem. Soc. 126*, 4167−4180.
80. Antosiewicz, J., McCammon, J. A., and Gilson, M. K. (1996) The Determinants of pK_as in Proteins, *Biochemistry 35*, 7819−7833.
81. Georgescu, R. E., Alexov, E. G., and Gunner, M. R. (2002) Combining conformational flexibility and continuum electrostatics for calculating pK_as in proteins, *Biophys. J. 83*, 1731−1748.
82. Rose, I. A., Fung, W. J., and Warms, J. V. B. (1990) Proton Diffusion in the Active Site of Triosephosphate Isomerase, *Biochemistry 29*, 4312−4317.
83. Harris, T. K., Abeygunawardana, C., and Mildvan, A. S. (1997) NMR Studies of the Role of Hydrogen Bonding in the Mechanism of Triosephosphate Isomerase, *Biochemistry 36*, 14661−14675.
84. Cleland, W. W., Frey, P. A., and Gerlt, J. A. (1998) The Low Barrier Hydrogen Bond in Enzymatic Catalysis, *J. Biol. Chem. 273*, 25529−25532.
85. Cleland, W. W. (2000) Low-barrier hydrogen bonds and enzymic catalysis, *Arch. Biochem. Biophys. 382*, 1−5.
86. Wierenga, R. K., Noble, M. E. M., and Davenport, R. C. (1992) Comparison of the refined crystal structures of liganded and unliganded chicken, yeast and trypanosomal triosephosphate isomerase, *J. Mol. Biol. 224*, 1115−1126.
87. Wierenga, R. K., Borchert, T. V., and Noble, M. E. M. (1992) Crystallographic binding studies with triosephosphate isomerases: conformational changes induced by substrate and substrate-analogs, *FEBS Lett. 307*, 34−39.
88. Rozovsky, S., and McDermott, A. E. (2001) The time scale of the catalytic loop motion in triosephosphate isomerase, *J. Mol. Biol. 310*, 259−270.
89. Johnson, L. N., and Wolfenden, R. (1970) Changes in absorption spectrum and crystal structure of triose phosphate isomerase brought about by 2-phosphoglycollate, a potential transition state analogue, *J. Mol. Biol. 47*, 93−100.
90. Wolfenden, R. V. (1970) Binding of Substrate and Transition State Analogues to Triosephosphate Isomerase, *Biochemistry 9*, 3404−3407.
91. Hartman, F. C., LaMuraglia, G. M., Tomozawa, Y., and Wolfenden, R. (1975) Influence of pH on the Interaction of Inhibitors with Triosephosphate Isomerase and Determination of the pK_a of the Active-Site Carboxyl Group, *Biochemistry 14*, 5274−5279.
92. Campbell, I. D., Jones, R. B., Kiener, P. A., Richards, E., Waley, S. C., and Wolfenden, R. (1978) The form of 2-phosphoglycollic acid bound by triosephosphate isomerase, *Biochem. Biophys. Res. Commun. 83*, 347−352.
93. Komives, E. A., Lougheed, J. C., Liu, K., Sugio, S., Zhang, Z., Petsko, G. A., and Ringe, D. (1995) The Structural Basis for Pseudoreversion of the E165D Lesion by the Secondary S96P Mutation in Triosephosphate Isomerase Depends on the Positions of Active Site Water Molecules, *Biochemistry 34*, 13612−13621.
94. Komives, E. A., Lougheed, J. C., Zhang, Z., Sugio, S., Narayana, N., Xuong, N. H., Petsko, G. A., and Ringe, D. (1996) The Structural Basis for Pseudoreversion of the H95N Lesion by the Secondary S96P Mutation in Triosephosphate Isomerase, *Biochemistry 35*, 15474−15484.
95. Zhang, Z., Komives, E. A., Sugio, S., Blacklow, S. C., Narayana, N., Xuong, N. H., Stock, A. M., Petsko, G. A., and Ringe, D. (1999) The Role of Water in the Catalytic Efficiency of Triosephosphate Isomerase, *Biochemistry 38*, 4389−4397.

BI047954C